Fifth International Conference

MMM 2010

Multiscale Materials Modeling

October 04 - 08, 2010, Freiburg, Germany

CONFERENCE PROCEEDINGS

Editors:
Peter Gumbsch
Erik van der Giessen

FRAUNHOFER VERLAG

Organized by Fraunhofer Institute for Mechanics of Materials IWM.
Hosted by University of Freiburg.

Fraunhofer IWM

UNI FREIBURG

Supported by

M2i Materials innovation institute

DFG Deutsche Forschungsgemeinschaft

Statistical Approaches

Complexity in Time-dependent Materials Deformation

Mikko Alava[1], Juha Koivisto[1], Lasse Laurson[2], Amandine Miksic[1] . and Jari Rosti[1]

[1]Aalto University, Department of Applied Physics, PO Box. 14100, 00076 Aalto, Finland
[2]ISI Foundation, Viale Settimo Severo 65, 10133 Torino, Italy
[1]email: Mikko.Alava@tkk.fi

The creep, fatigue, and relaxation of materials under external loads or when such are removed is a long-standing problem in materials science. Quite a few empirical scaling laws have been established for all these ranging from the Andrade's law for primary (power-law) creep to the Basquin law for cyclic loading or fatigue. In this work, we review experiments and comparisons with theoretical ideas to understand possible signatures of correlated dynamics in all these.

In primary and secondary creep, we discuss the role and importance of strain rate fluctuations – how localized the creep deformation is actually. This is augmented with the application of the theory of absorbing state phase transitions to understand and summarize the observations. Similar ideas prove useful to grasp the essentials of creep strain relaxation. The competition of loading and relaxation is best brought forward in low-cycle fatigue failure, which compares best with simple creep. We discuss evidence for a Grant-Monkman law (linear relationship) between the minimum strain-rate and the sample lifetime. In our investigations, the main experimental techniques are Acoustic Emission detection for observing damage mechanics and Digital Image Correlation to look at local strain (rate) fields and to observe with high accuracy the sample deformation.

Damage and dissipation mechanisms in the dynamic fracture of brittle amorphous materials: Velocity driven transition from nominally brittle to quasi-brittle

D. Bonamy[1,a], J. Scheibert[1,2], C. Guerra[1,3] and D. Dalmas[2]

[1] CEA, IRAMIS, SPCSI, Group Complex Systems and Fracture, F-91191 Gif-sur-Yvette, France
[a.] email : daniel.bonamy@cea.fr
[2.] Unité Mixte CNRS/Saint-Gobain, Surface du Verre et Interfaces, 39 Quai Lucien Lefranc, 93303 Aubervilliers cedex, France
[3.] Universidad Autonoma de Nuevo Leon, San Nicolas de los Garza, Mexico.

Crack propagation is the basic mechanism responsible for the brutal failure of brittle materials. Over the past century, a coherent theoretical framework, the so-called Linear Elastic Fracture Mechanics (LEFM) has developed [1]. LEFM provides an equation of motion that relates the crack speed to the stress intensity factor. This equation of motion brings into play a third quantity, so-called fracture energy Γ; that is the energy required for the moving crack to expose a unit area of cracked surface. In brittle materials, the fracture energy is constant and the maximum crack velocity is predicted to be the Rayleigh wave speed, c_R. Many experiments show that neither of these predictions is verified [2].

To unravel the origin of this discrepancy, we performed dynamic fracture experiments on polymethylmethacrylate (PMMA), the archetype of nominally brittle materials, and we measured Γ over a wide range of crack velocities [3]. At small velocities, Γ is constant and equal to that at crack initiation, as predicted by LEFM. But above a well defined velocity $v_a = 0.2c_R$, Γ trebles suddenly. Simultaneously, conic patterns start to appear on the fracture surfaces. Above v_a, both Γ and the conics density increases with the crack speed. The fracture energy diverges when the speed reaches about $0.5\ c_R$.

In many materials, the conic patterns are interpreted as the signature of the nucleation, growth and coalescence of micro-cracks ahead of the main crack front. Hence, at velocity greater than $v_a = 0.2\ c_R$, crack propagation in PMMA comes with microfracturing events, *as in quasi-brittle materials*. A simple scenario allows to relate energetic and fractographic measurements. It suggests that dynamic fracture in brittle amorphous materials is controlled by the velocity driven brittle/quasi-brittle transition evidenced here.

[1] L. Freund, Dynamic Fracture Mechanics (Cambridge University Press, Cambridge, England, 1990)
[2] K. Ravi-Chandar, Dynamic Fracture (Elsevier, Amsterdam, The Netherlands, 2004)
[3] J. Scheibert, C. Guerra, F. Célarié D. Dalmas, D. Bonamy, Phys. Rev. Lett. **104** 045501 (2010)

STRESS CORROSION FRACTURE OF SILICATE GLASSES: HOW FAR CAN WATER PENETRATE?

F. Lechenault[1], F. Cousin[2], C. Rountree[3], E. Bouchaud[1,4]

[1-3] *CEA-Saclay, 91191 Gif-sur-Yvette Cedex, France*
[1] *Service de Physique de l'Etat Condensé (SPEC)*
[2] *Laboratoire Léon Brillouin (LLB)*
[3] *Service de Physique et Chimie des Surfaces et Interfaces (SPCSI)*
[4] *Norwegian University of Science and Technology (NTNU), Department of Physics, Trondheim, Norway*

Although glass can be considered as homogeneous at scales as small as a few tens of nanometers, since it exhibits no density fluctuations beyond, its amorphous structure makes it a disordered material with respect to fracture properties. Fluctuations of the binding energies and of the orientations of Si-O bonds with respect to the external stress make it unlikely that bonds closest to the crack tip break first, despite the high stress concentration. As a consequence, glass behaves in a quasi-brittle manner rather than in a purely elastic way, although it is of course deprived of intrinsic plasticity beyond one nanometer [1].

In situ Atomic Force Microscopy (AFM) experiments tracking the slow progression of a stress corrosion crack seemed to show indeed the opening and growth of nano size flaws ahead of the tip [2,3]. Furthermore, glass fracture surfaces reveal the same morphology as the one of quasi-brittle materials such as mortar or wood [4].

However, these results are highly controversial, and, as a matter of fact, artifacts may seriously affect AFM observations, both *in situ* [5] and *post mortem* [6]. Furthermore, the low diffusion coefficient of water in silica should forbid hydrolysis at a distance from the crack tip, except at the free surface. Our recent neutron reflectivity experiments show that water actually penetrates into the material during stress corrosion fracture. Comparing two experiments performed for different crack velocities shows that the diffusion coefficient is hugely increased under stress, allowing for bond breakings at several tens of nanometers ahead of the main crack tip.

1. C. L. Rountree, M. Talamali, D. Vandembroucq, E. Bouchaud, S. Roux, *Phys. Rev. Lett.* ***102***, 195501 (2009)
2. F. Célarié, S. Prades, D. Bonamy, L. Ferrero, E. Bouchaud, C. Guillot, C. Marlière, *Phys. Rev. Lett.* ***90***, 075504-1 (2003)
3. S. Prades, D. Bonamy, D. Dalmas, E. Bouchaud, C. Guillot, *Int. J. of Solids & Structures* **42**, 637-645 (2004)
4. L. Ponson, D. Bonamy, E. Bouchaud, Phys. Rev. Lett. **96**, 035506 (2006)
5. J. Lopez-Cepero, S. M. Wiederhorn, Th. Fett, J.-P. Guin, *Int. Mat. Res.* ***98***, (2007)
6. F. Lechenault, G. Pallares, M. George, C. Rountree, E. Bouchaud, and M. Ciccotti, *Phys. Rev. Lett.* ***104***, 025502 (2010)

Morphological aspects and deterministic reconstruction of dynamical fracture surfaces in brittle materials

D. Dalmas[1,a], C. Guerra[2,3], J. Scheibert[2] and D. Bonamy[2]

[1] Unité Mixte CNRS/Saint-Gobain "Surface du Verre et Interfaces" UMR 125, BP 135, F-93303, Aubervilliers, Cedex, France.
[2] CEA, IRAMIS, SPCSI, Grp. Complex Systems & Fracture, F91191 Gif sur Yvette, France.
[3] Universidad Autonoma de Nuevo Leon, San Nicolas de los Garza, Mexico.
[a] e-mail: davy.dalmas@saint-gobain.com

Linear Elastic Fracture Mechanics (LEFM) provides a quantitative description of the crack motion that agrees well with observations in brittle materials as long as the crack growth is sufficiently slow. However, several issues remain unsolved: (i) experimental observations reveal that at high velocity, the crack speed is systematically smaller than the one predicted by LEFM [1] and (ii) above a given velocity, roughening of fracture surfaces is observed.
In this work, we show how one can reconstruct deterministically the micrometer/microsecond damage and failure processes involved in dynamic fracture from the morphology of fracture surfaces – Those have been obtained via a wedge splitting geometry which allows to make a dynamic crack grow in opening mode in Plexiglas while measuring its instantaneous velocity [2]. When this velocity is larger than 165 *m/s*, conic markings start to be observed on the surfaces. At higher velocities, the density of conics marks is increasing. Each conic mark is believed to result from the intersection of the main moving crack with a penny shaped micro-crack that nucleates ahead and grow radially. In such a model, the nucleation centre coincides with the conics focus and the nucleation distance coincides with the apex-focus distance of the conics. Based on this simple geometrical model, we have reconstructed the full dynamics of both the propagation of the moving crack front and that of microfracturing events. Their statistics has been characterized: spatial distribution of nucleation sites, time delay and nucleation distance between microfracturing events, intermittency in the propagation of the main crack front…. The understanding of the propagation and damage mechanisms through this deterministic reconstruction shed light on the origin of the discrepancy between theory and experiments at high velocities.

[1] L.B. Freund, *Dynamic Fracture Mechanics* (Cambridge University Press, New York 1990).
[2] J. Scheibert, C. Guerra, F. Célarié, D. Dalmas, D. Bonamy, Phys. Rev. Lett. **104**, 045501 (2010).

Statistics of Internal Stress of Dynamical Dislocation Ensembles**

Jie Deng and Anter El-Azab*

Department of Scientific Computing, Florida State University, Tallahassee, FL, USA

*Corresponding author. Florida State University, 400 Dirac Science Library, Tallahassee, FL 32306-4120. E-mail address: aelazab@fsu.edu

A computational technique to characterize the statistics of internal stress field of 3D dislocation systems in deforming crystals is presented. In this technique, 3D dislocation realizations are generated by the method of dislocation dynamics simulation and the associated internal stress is computed by solving the corresponding internal stress boundary value problem. The statistics of internal stress is modeled using probability density and pair correlation functions derived as the first order and second order moments for the internal stress with respect to a generalized probability density function of the underlying dislocation configuration. The results show that the stress components exhibit nearly symmetric probability density functions with zero mean values, which depend on the level of crystal strain. It is also shown that the probability density function of the resolved shear stress is skewed and has non-zero mean value. The correlation of all stress components and resolved shear stress are found to be highly anisotropic and tend to be enhanced as the crystal strain (and, in turn, the dislocation density) is increased due to the enhanced fluctuations of the internal stress. For this reason, the connection between the dislocation density fluctuations and internal stress fluctuations is also analyzed as part of the current investigation.

** Research supported by the U.S. Department of Energy, Office of Basic Energy Sciences, Division of Materials Sciences and Engineering

Intermittent Flow in Microcrystal Plasticity

Dennis M. Dimiduk[1], Edward M. Nadgorny[2], Chris Woodward[1], Michael D. Uchic[1], Paul Shade[3], Satish I. Rao[4], Stefanos Papanikolaou[5] and James Sethna[5]

[1]Air Force research Laboratory, Materials and Manufacturing Directorate, AFRL/RXLM, Bldg. 655, 2230 10th Street, Wright-Patterson AFB, OH 45433-7817, USA, dennis.dimiduk@wpafb.af.mil
[2]Michigan Technological University, Department of Physics, Houghton, MI 49931 USA
[3]UTC, 1270 N. Fairfield Rd., Dayton, OH 45432-2600, USA
[4]UES, Inc., 4401 Dayton-Xenia Road, Dayton, OH 45432-1894, USA
[5]Cornell University, Department of Physics, Ithica, NY 14853-2501, USA

Experimental studies of a variety of materials, as well as dislocation dynamics simulations, show both macroscopic (temporal evolution of acoustic emission, slip line and strain burst magnitudes [1,2,3]) and microscopic (displacement-time history during microsample compression testing and simulation [4,5,6]) evidence of intermittency during plastic deformation. Also, the studies show that intermittency revealed by both the magnitude and duration of displacement events exhibits scale-free regimes. Idealized models of dislocation ensemble interactions provide phenomenological explanations of the experiments via a mean-field theory of elastic surface depinning transitions [1,6]. While several past investigations are consistent with mean-field theory, experimental deviations from the theory were also observed for scale-free flow at different strain rates or for selected materials. The present studies further investigate the intermittent flow in microsamples of LiF and pure Ni single crystals. Effects of strain rate, sample size and flow stage are evaluated to gain further insights into the mechanisms of intermittency and its connections to current or refined models. The results and their evaluation emphasize the need to understand dislocation multiplication and its ties to intermittent flow in not only microscopic but also macroscopic deforming samples.

[1] M.C. Miguel, A. Vesignani, S. Zapperi, J. Weiss, and J-R. Grasso, Nature (2001) 410, 667.
[2] J. Schwerdtfeger, E. Nadgorny, V. Koutsos, J.R.Blackford and M. Zaiser, Phil Mag. (2010) submitted for publication.
[3] C. Fressengeas, A.J. Beaudoin, D. Entemeyer, T. Lebedkina, M. Lebyodkin and V. Taupin, Phys. Rev. B (2009) 79, 014108.
[4] D.M. Dimiduk, Science (2006) 312, 1188.
[5] D.M. Dimiduk, Phil. Mag. (2010) in press.
[6] M. Zaiser and P. Moretti, J. Stat. Mech. (2005) 8, P08004.

On the role of short-range vs. long-range spatial correlations in dislocation patterning

Juliette Chevy[1], Claude Fressengeas[2], Mikhail Lebyodkin[2], Vincent Taupin[2], Pierre Bastie[3], Paul Duval[4]

[1]Department of Mechanical Science and Engineering,
University of Illinois at Urbana-Champaign, 1206 W. Green St., Urbana, IL 61801, USA
[2]Laboratoire de Physique et Mécanique des Matériaux,
Université Paul Verlaine – Metz / CNRS, Ile du Saulcy, 57045 Metz Cedex, FRANCE
[3]Institut Laue – Langevin, BP 156, 38042 Grenoble Cedex 9, FRANCE
[4]Laboratoire de Glaciologie et Géophysique de l'Environnement – CNRS 54 rue Molière,
38402 Sant Martin d'Hères, FRANCE
e-mail : claude.fressengeas@univ-metz.fr

Hard X-ray diffraction experiments have provided evidence of a strongly heterogeneous distribution of dislocation densities along the axis of cylindrical ice single crystals oriented for basal slip in torsion creep [1]. The dislocation arrangements showed a complex scale-invariant character, which was analyzed by means of statistical and multifractal techniques. A trend to decreasing autocorrelation of the dislocation distribution was observed as deformation proceeds. At low strain levels, long-range spatial correlations control the dislocation distribution, but short-range correlations in relation with cross-slip activated by internal stresses progressively prevail when strain increases. This trend was reproduced by a generic model based on field dislocation dynamics, a theory accounting for both long-range elastic interactions and short-range interactions through transport of dislocation densities [2]. The results suggest that dislocation patterning is controlled by short range interactions at sufficiently large strains, although their contribution to work hardening is not as decisive.
.

[1] J. Chevy, C. Fressengeas, M. Lebyodkin, V. Taupin, P. Bastie, P. Duval, Acta Mater. **58** (2010) 1837-1849.
[2] A. Acharya, A. Roy, J. Mech. Phys. Solids, **54** (2006) 1687-1710

Accurate description of elastic properties of random alloys with minimum supercell sizes

Martin Friák[1*], Johann von Pezold[1], Alexey Dick[1] and Jörg Neugebauer[1]

[1]Max-Planck-Institut für Eisenforschung GmbH, Max-Planck-Strasse 1, D-40237, Düsseldorf, Germany ([*]m.friak@mpie.de)

The atomistic description of random alloys has been the subject of intense research efforts over the last 20 years, which led to the development of three alternative methods: cluster expansion (CE), special-quasi-random structures (SQS), and the coherent potential approximation (CPA). The CPA accounts for the randomness in these structures in a mean-field approach, which limits its applicability to alloys consisting of chemically and elastically similar constituents. CE methods and quasi random structures have both originally been developed with the aim of an energetic description of random alloys. While the CE method has recently been extended to also account for elastic properties, the description of elastic properties by SQS has not been systematically studied so-far. To this end we developed a set of system-independent 32-atom fcc SQS and determined C_{11}, C_{12}, and C_{44} of AlTi solid solutions over the entire concentration range, using both the SQS and supercells containing randomly generated Ti distributions within the Al matrix consisting of up to 4000 atoms. The elastic properties of these alloys could be described using the set of SQS with an accuracy comparable to the accuracy achievable by randomly generated impurity distributions within 3x3x3 108 atomic (C_{44}) and 4x4x4 256 atomic (C_{11} and C_{12}) fcc supercells, irrespective of the impurity concentration. The smaller system size makes the proposed SQS structures ideal candidates for the *ab initio* determination of the elastic constants of random substitutional alloys.

Statistical properties of the plastic response of submicron size specimen

Péter D. Ispánovity[1,2], István Groma[1], Géza Györgyi[1,3] and Daniel Weygand[4]

[1] Eötvös University Budapest, Department of Materials Physics, PO BOX 32, 1518 Budapest, Hungary

[2]Paul Scherrer Institute, CH-5232 Villigen PSI, Switzerland.

[4]Karlsruhe Institute for Technology, izbs, Kaiserstraße 12, D-76131 Karlsruhe, Germany.

[3]e-mail:gyorgyi@glu.elte.hu

The existence of a specific yield stress, where a macroscopic piece of crystal begins to easily flow, has been one of the basic observations of material science. Recent experimental investigations and computer simulations revealed that plastic flow in submicron size specimens is not a smooth process. It is characterised by intermittent, unpredictable bursts of activity manifested in dislocation avalanches. This feature bears a close resemblance to the behaviour of a variety of self-organised critical systems, like granular matter or vortices in superconducting films. Avalanches become more pronounced, if the size of the specimen goes below micron, where fluctuations are large prohibiting the identification of a sharp yield stress. Here we study by simulation, in 2D and 3D, the evolution of dislocation systems in submicron objects under increasing stress. We show that while the stress-strain relation of individual samples exhibits jumps, its average and mean deviation still specify a well-defined critical stress. An in depth study of the velocity distribution of individual short dislocation segments shows that it undergoes a specific transition at the same yield stress level between the jammed and the flowing state. Furthermore, we find that the tail of the distribution of velocities displays a universal inverse cubic power decay, attributed to dislocation avalanches. We conclude that for avalanches the only important driving force is the long-range stress field of dislocations, so they are hardly affected by short-range effects. Because of the universal nature of our results they may also help understanding avalanche-like fluctuations in other highly coupled systems.

Toward a continuum theory of dislocations

István Groma[1], Géza Györgyi[1] and Péter D. Ispánovity[1,2]

[1] Eötvös University Budapest, Department of Materials Physics, PO BOX 32, 1518 Budapest, Hungary

[2]Paul Scherrer Institute, CH-5232 Villigen PSI, Switzerland.

[1]e-mail: groma@metal.elte.hu

Over the past decade, there has been a increasing activity to develop a continuum theory of dislocations applying statistical physics methods. The theoretical investigations are largely motivated by recent experimental findings like if the characteristic size of a specimen is less than about 10 μm the plastic response of the crystalline materials depends on the size (size effect).

In the talk presented, after a short summary of recent different approaches in continuum theory of dislocations, the following issues are discussed:

- Different variational approaches the get the stress state of a material containing topological defects [1]. The concept of “plastic potential”.
- Beyond the classical Volterra theory of dislocation. Incorporating core effects and anharmonicity [2].
- Can we handle large deformations?
- Role of dislocation-dislocation correlation. The origin of the “back” stress [1].
- Stress screening due to induced GND [3].
- Time evolution of the different dislocation densities. A phase field approach [1].
- Time evolution of the dislocation velocity distribution. Scaling properties.
- On the dynamics of the dislocation-dislocation correlation function. Linear response theory [4].
- Role of fluctuations. Long versus short range dislocation-dislocation interaction.

[1] Groma I, Gyorgyi G, Kocsis B, Dynamics of coarse grained dislocation densities from an effective free energy, Phil. Mag. **87**, 1185-1199 (2007)

[2] Groma I, Ispanovity PD, Role of elastic anharmonicity in dislocation patterning,

Phys. Rev. B **76** , 054120 (2007)

[3] Groma I, Gyorgyi G. Kocsis B., Debye screening of dislocations, Phys. Rev. Letter, **96**, 165503 (2006)

[4] Ispanovity PD, Groma I, Gyorgyi G, Evolution of the correlation functions in two-dimensional dislocation systems, Phys. Rev. B **78**, 024119 (2008)

Slip avalanches in a fiber bundle model

Ferenc Kun[1], Zoltán Halász[2] and Zsuzsa Danku[1]

[1]Department of Theoretical Physics, University of Debrecen
P.O.Box.:5, H-4010 Debrecen, Hungary, Email: feri@dtp.atomki.hu
[2]Institute of Nuclear Research, P.O.Box.: 51, H-4005 Debrecen, Hungary

We investigate the emergence of crackling noise in heterogeneous materials which respond to an increasing external load by local rearrangements with stick-slip mechanism. We consider a fiber bundle model where over-stressed fibers do not break instead they increase their relaxed length in a slip event until they can sustain the load. The system is driven by small load increments giving rise to the slip of a single fiber which may then trigger an entire avalanche of slip events due to load redistribution in the bundle.

We show by analytic calculations and computer simulations that the load increment triggering the slip bursts, furthermore, the number of slipping fibers and the total slip length of the bundle are all characterized by power law distributions. We demonstrate that the amount of disorder and the total number of allowed slips play a crucial role in the system: a disorder induced phase transition is obtained from a low disorder phase where the system snaps with macroscopic bursts to the high disorder one where only small avalanches pop up. Our model provides an adequate description of the micromechanics of disordered systems which store hidden length [1,2].

Recently, it has been shown in [3] that the mode of external driving has a crucial effect on the critical non-equilibrium steady states in slowly driven bistable heterogeneous systems with controllable disorder: changing the driving from soft to hard a crossover is obtained from the classical order-disorder universality class to the quenched Edwards-Wilkinson class of SOC type. In our investigations of the avalanche statistics only stress controlled loading is considered, which corresponds to the perfectly soft driving of [3]. We construct the phase diagram of our system, which can be considered as an extension of the zero softness part of the phase diagram of [3] with the additional degree of freedom of varying the number of stable configurations under an infinite range of interaction.

References

[1] Z. Halász and F. Kun, Phys. Rev. E **80**, 027102 (2009).
[2] Z. Halász and F. Kun, Europhys. Lett. **89**, 26008 (2010).
[3] F.-J. Perez-Reche, L. Truskinovsky, and G. Zanzotto, Phys. Rev. Lett. **101** 230601 (2008).

Dynamical correlations near dislocation jamming

Lasse Laurson[1], M.-Carmen Miguel[2] and Mikko J. Alava[3]

[1]ISI Foundation, Viale S. Severo 65, 10133 Torino, Italy
[2]Departament de Física Fonamental, Facultat de Física, Universitat de Barcelona, Diagonal 647, 08028 Barcelona, Spain
[3]Aalto University, Department of Applied Physics, PO Box 14100, 00076 Aalto, Espoo, Finland

The dynamical behavior of crystalline solids subject to an external shear stress is controlled by the existence of a finite yield stress, separating a low stress phase with only elastic or reversible deformation from a high stress phase with sustained plastic or irreversible deformation mediated by dislocation motion. While concepts such as depinning and/or jamming transitions of the dislocation assemblies have been discussed before in an effort to comprehend the characteristics of this yielding transition, its precise nature still remains to be ascertained.

In this work [1] we study the heterogeneous and collective nature of dislocation dynamics within a crystal plasticity or discrete dislocation dynamics model with a single slip geometry. In particular, we consider the first-passage properties of the dislocation dynamics close to the yielding transition. As the transition is approached from the moving phase, the first-passage time distribution exhibits scaling, and the stress dependence of a related peak *dynamical* susceptibility is characterized by a power law divergence. We relate this scaling to a mean field - like avalanche description of the dynamics. While the static structural correlations are found to be independent of the external stress, we identify a diverging dynamical correlation length in the direction perpendicular to the dislocation glide motion. Thus, our results indicate that the yielding transition of crystalline solids is indeed a second order phase transition characterized by a divergent dynamical susceptibility and an associated correlation length, and that the concept of jamming can be successfully applied to understand the characteristics of the transition, analogously to many other systems such as granular materials and molecular liquids.

[1] Lasse Laurson, M.-Carmen Miguel, and Mikko J. Alava, arXiv:1002.2587.

Statistical Distributions of Stresses within Plastically Deformed Copper: Models, Simulations and Microbeam X-ray Measurements

Lyle Levine[1], Peter Geantil[2], Bennett Larson[3], Francesca Tavazza[1], Jonathan Tischler[2], Wenjun Liu[4], Michael Kassner[2]

[1]Materials Science & Engineering Laboratory, National Institute of Standards and Technology, Gaithersburg, Maryland, 20899-8553, USA; Lyle.Levine@nist.gov
[2]Department of Aerospace and Mechanical Engineering, University of Southern California, Los Angeles, California 90089, USA
[3]Materials Science & Technology Division, Oak Ridge National Laboratory, Oak Ridge, Tennessee 37831, USA
[4]Advanced Photon Source, Argonne National Laboratory, Argonne, Illinois 60439-4800, USA

Over the past thirty years, there has been considerable disagreement concerning the existence and magnitude of long range elastic strains (and therefore stresses) in plastically deformed metals. Recent synchrotron X-ray measurements using depth resolved, sub-micrometer X-ray beams have confirmed the presence of these strains and found that the cell interior strains are compressive in the unloaded tension samples and tensile in the unloaded compression samples.[1] The strains also exhibit large cell-to-cell variations that have important implications for theories of dislocation structure evolution, dislocation transport, changes in mechanical properties during reverse loading (Bauschinger effect and fatigue) and the extraction of dislocation structure parameters from X-ray line profiles.

Here, we report extensive measurements of elastic strains within individual dislocation cell walls and adjacent cell interiors in plastically deformed copper; the corresponding cell wall and cell interior stress distribution functions will be described. Two viable mechanisms for the origin of these distribution functions have been identified: size effects arising from the dipolar nature of the stress field and stochastic processes operating during the evolution of individual dislocation walls. Analytic models for both processes will be presented and compared with the measured elastic strains. Finally, a three dimensional computational model based upon random trapping of dislocations on dislocation cell walls will be examined. The stress distributions produced by these trapped dislocations will examined as a function of a wide variety of physical parameters, such as the average number of excess dislocations, average cell size, cell size distribution, and wall thickness.

1. L. E. Levine *et al*., *Nature Materials*, **5**, 619-622 (2006).

A vortex crystal that flows like a liquid: Grain-boundary scars in flat geometry

M. Carmen Miguel[1], Adil Mughal[2] and Stefano Zapperi[2,3]

[1]Departament de Física Fonamental, Facultat de Física, Universitat de Barcelona
Av. Diagonal 647, 08028 Barcelona, Spain, email: carmen.miguel@ub.edu
[2]ISI Foundation, Viale San Severo 65, 10133 Torino, Italy
[3]CNR-IENI, Via R. Cozzi 53, 20125 Milano, Italy

We investigate the structural transformations of a vortex crystal in the Corbino disk geometry in response to an injected current in the superconducting material. At high enough currents, the vortex crystal exhibits a laminar flow response, with a velocity profile decaying in the same manner as the driving current, as if we were dealing with an uncorrelated vortex liquid phase. Laminar flow can be induced by thermal fluctuations melting the crystal, but also by applying a large current at zero temperature. While the flow profile is the same in the two cases, the underlying vortex structure is completely different. Here we show that in the Corbino disk geometry, a polycrystalline vortex structure flows in a liquid-like manner due to the presence of disclinations and dislocations that induce the necessary curvature in the host crystal. Disclinations in this flat geometry migrate from the sample boundary to the interior of the crystal assisted by the formation of grain-boundary scars, i.e. walls of equally charged dislocations emanating from boundary disclinations. The problem of ground-state configurations including stable grain boundary scars on (positively or negatively) curved surfaces has recently attracted new consideration. Here we show that these topological structures, which in equilibrium conditions would be forbidden in flat geometry, can otherwise be induced and maintained by shear stress. We provide an estimate of the critical current needed to initiate the formation of grain boundary scars in the Corbino disk geometry, and thus to sustain the laminar flow of the vortex crystal, and show that the result is in good agreement with numerical simulations of the vortex array.

Statistical Modeling of Elastic Strain, Lattice Rotation and Dislocation Density Tensor in FCC Crystals

Mamdouh Mohamed[1], Jie Deng[2], Anter El-Azab[1]* and B. C. Larson[3]

[1] Department of Scientific Computing, Florida State University, Tallahassee, FL, USA
[2] Currently with Sandia National Laboratories, Livermore, CA, USA
[3] Materials Sciences and Technology Division, Oak Ridge National Laboratory, Oak Ridge, TN, USA
*** Corresponding author. E-mail address: aelazab@fsu.edu**

ABSTRACT

A computational technique is developed to simulate the statistics of internal elastic fields of 3D dislocation systems in deforming crystals. The internal elastic fields are computed based on 3D dislocation realizations generated by the method of dislocation dynamics simulation. The results show that the dislocation density tensor components exhibit nearly symmetric probability density functions with zero mean values. The probability density function of the lattice rotation is found to be nearly symmetric, but with nonzero mean. The radial correlation of dislocation density tensor and lattice orientation showed slow decay followed by slight oscillatory behavior with correlation and anti-correlation regimes. The importance of the current analysis is discussed in relation to mesoscale plasticity model development and to direct comparison of simulations with spatially resolved 3D X-ray microscopy measurements of lattice rotation and the dislocation density tensor.

1. Introduction

Plastic deformation leaves crystals highly dislocated. The dislocation state of a crystal evolves with deformation and it determines the hardening behavior of the crystal during the deformation process. In addition to the density of dislocations, the internal fields of these dislocations represent the main signature of the dislocation structures that can be probed experimentally. The geometrical fields in particular, namely the lattice rotation and elastic strain, are important because they can reveal important information about the dislocation state itself. For example, these fields can be used to compute the dislocation density tensor, a key geometric measure for the dislocation system in distorted crystals [1]. X-ray microscopy currently provides spatially resolved measurements of local lattice orientation and dislocation density tensor in 3D and with sub-micron scale resolution [2, 3]. The ability to reveal such detailed microstructure information provides a previously missing bridge between mesoscale deformation experiments and computer simulations results. This short communication outlines the procedure to calculate the elastic strain and lattice rotation fields (and dislocation density tensor) in highly dislocated crystals, starting with dislocation configurations extracted from dislocation dynamics simulations [4]. The statistical behavior of these fields, described in terms of probability density and pair correlations functions, is investigated, as a step towards comparison between mesoscale simulations and experiments. Preliminary results from simulations are briefly discussed in this communication.

2. Theoretical Modeling

The elastic strain and lattice rotation fields of dislocations inside a finite crystal volume have two contributions. The first contribution is the so-called infinite-medium contribution, which

comes from the classic line-integral form of the elastic solution of dislocations inside an infinite medium [5]. We are here adopting the non-singular expressions developed later by Cai and co-workers [6]. The second contribution is called the image field, which accounts for the effect of the physical boundary of the crystal, or the field of dislocations residing outside a crystal volume of interest (e.g., the dislocation dynamics simulation volume). The image field is calculated by solving a traction boundary value problem [7]. Once at hand, these two contributions can be used to calculated the dislocation density tensor according to the continuum theory of dislocations [1]; the dislocation density tensor can be found from

$$\alpha_{ij} = \kappa_{ji} - \delta_{ij}\,\kappa_{kk} - e_{ikl}\,\partial_k \varepsilon_{lj}\,, \tag{1}$$

where δ_{ij} is the Kronecker delta, e_{ikl} is the permutation symbol, and κ_{ij} is the lattice curvature tensor defined as the gradient of the lattice orientation $\kappa_{ij} = \partial_i \theta_j$, and θ_j is the lattice rotation, defined in terms of the lattice rotation field as $\omega_{ij} = e_{ijk}\theta_k$.

The internal elastic fields and dislocation density tensor possess statistical characteristics due to the discrete nature of dislocations. A probability density function (PDF) and a pair correlation function are used to demonstrate this statistical behavior. Expressions for both statistical quantities were shown before [8].

3. Numerical Simulation

The dislocation dynamics code microMegas [4] was used to simulate single crystal deformation, and several dislocation configurations were extracted for statistical analysis. A copper crystal, with simulation box size *L* of 5 microns was loaded under constant strain rate of 25 $\sec^{-1}$ in the [001] direction. The resulting dislocation configurations were then fed into a finite element code to calculate the image contribution of the internal elastic fields, which is then added to the infinite contribution to evaluate the total internal elastic fields. For these calculations, the simulation volume was divided into (50×50×50) volume elements, and the internal elastic fields were evaluated in the middle of each volume element as the average over (3×3×3) Gauss points inside the volume element. The gradients of the elastic strain and lattice rotation fields were then calculated via centered difference formula, in order to evaluate the dislocation density tensor, as was shown in Eqn. (1). During radial correlation calculations, the absolute value of difference in Cartesian coordinates Δx, Δy, and Δz was confined to be less than 0.75*L*, to avoid the edge effect.

4. Results and Discussion

Previous results showed a symmetric PDF for both internal stress and elastic strain, with zero mean [8]. This is consistent with the fact that dislocation stress in a bounded crystal is traction free, and it implies that the internal elastic strain is the same as its own fluctuation. Here, we focus on the statistics of lattice rotation and dislocation density tensor at (plastic) strain level of 2.3%. Figure 1 (a) shows the PDF for the three lattice rotation components. The figure shows a nearly symmetric shape for the probability, but with nonzero mean. So, unlike the symmetric part of displacement gradient, the antisymmetric part seems to have a nonzero volume average (ensemble average), which means that crystal lattice has a net misorientation in a certain direction due to the existence of dislocations.

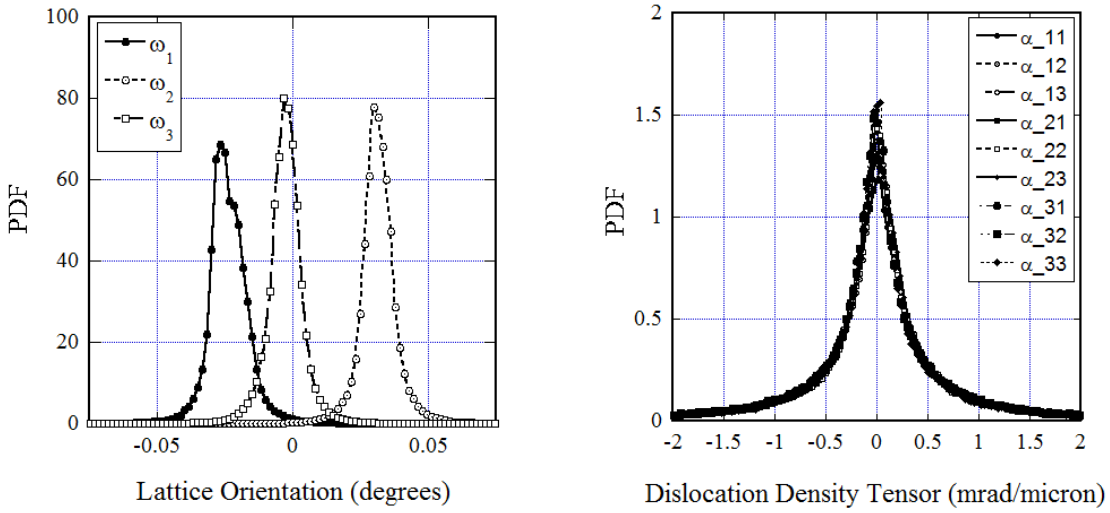

(a) (b)

Figure 1. (a) Probability density function for lattice orientation. (b) Probability density function for dislocation density tensor components.

Figure 1 (b) shows the PDF for the dislocation density tensor components. The figure shows that all the components of the dislocation tensor have almost the same distribution. The zero mean value of the distribution suggests that the dislocation configuration has a zero net Burgers vector, which coincides with the fact that the input configuration for the dislocation dynamics simulation consisted of a set of square loops, and applying periodic boundary conditions throughout the simulation kept this zero net Burgers vector.

Figure 2 (a) and (b) show the radial pair correlation function for the lattice orientation and the trace norm of the dislocation density tensor, respectively. Both correlations decay to zero (no correlation) value and then show slight oscillations about that value. The oscillation of the correlation of the trace norm of the dislocation density tensor implies the formation of cell structure during deformation, which is revealed by 3D maps of the trace norm itself.

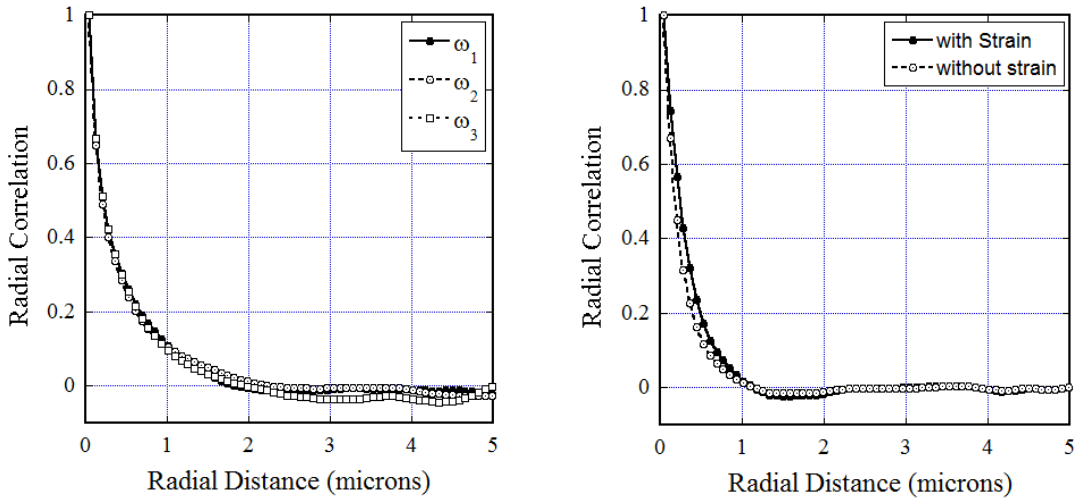

(a) (b)

Figure 2. (a) Radial correlation of the lattice rotation. (b) Radial correlation of the trace norm of dislocation density tensor.

It has been shown that the elastic strain gradient term in Eqn. (1) contributes significantly to the probability distribution function of the components and the trace norm of the dislocation density tensor (results omitted due to limited space). Figure 2 (b), however, shows that the radial correlation of the trace norm of the dislocation density tensor, computed with and without the strain gradient contribution, is approximately the same. This suggests that the strain gradient and curvature contributions to dislocation density tensor have similar radial correlations, which is consistent with previously published results on 3D correlation of the dislocation density components [8].

5. Concluding Remarks

A preliminary investigation for the statistical analysis of internal elastic fields and dislocation density tensor has been conducted. The statistical characteristics of these fields were revealed via probability density, pair correlation function and 3D maps (not shown here). The results show a symmetric distribution of the lattice orientation, with nonzero mean value. The distribution of the dislocation density tensor components was symmetric, which is consistent with the simulated dislocation structure. The radial correlation functions for lattice rotation and dislocation density tensor exhibit initial decay followed by slight oscillations about no-correlation values. The results, along with 3D maps of the trace norm of the dislocation density tensor, indicate the formation of cell structure. Additional results will be presented at the conference.

Acknowledgements

Research sponsored by the Division of Materials Sciences and Engineering, Office of Basic Energy Sciences, U.S. Department of Energy; ORNL UT-Battelle contract DE-AC05-00OR22725; Florida State University contract DE-FG02-08ER46494.

References

[1] E. Kroner, "Continuum theory of defects," in Physics of Defects, Edited by R. Balian, M. Kleman and J. Poirier (North-Holland, Amsterdam 1981) pp. 282-315.
[2] B. C. Larson, W. Yang, G. E. Ice, J. Budia, and J. Z. Tischler, "Three-dimensional X-ray structural microscopy with submicrometre resolution," Nature, **415**, 887 (2002).
[3] B. C. Larson, A. El-Azab, W. Yang, J. Z. Tischler, W. Liu, and G. E. Ice, "Experimental characterization of the mesoscale dislocation density tensor," Philosophical Magazine, **87**, 1327 (2007).
[4] B. Devincre, "Mesoscale simulation of the dislocation dynamics," Computer Simulation in Materials Science, Edited by H. Kirchner, V. Pontikis, L. Kubin (Kluwer, Dordrecht 1996), pp. 309-323.
[5] J. Hirth and J. Lothe, Theory of Dislocations (John Wiley & Sons, New York 1982).
[6] W. Cai, A. Arsenlis, C. Weinberger, V. Bulatov, "A non-singular continuum theory of dislocations," Journal of the Mechanics and Physics of Solids, **54**, 561 (2006).
[7] Anter El-Azab, "The boundary value problem of dislocation dynamics," Modeling and simulation in Materials Science and Engineering, **8**, 37 (2000).
[8] J. Deng, A. El-Azab, and B. C. Larson, "Statistics of internal elastic fields and dislocation density tensor in deformed FCC crystals," in MRS Symposium Proceedings, 1130E (Warrendale, PA, Materials Research Society 2009), paper number 1130-W12-11, pp. 1-6.

Yield and scale-invariance in plastic flow of sub-microscale crystalline materials

Paolo Moretti[1,2], Benedetta Cerruti[2,3] and M. Carmen Miguel[2]

[1]Departament de Física i Enginyeria Nuclear
Universitat Politècnica de Catalunya - BarcelonaTech
Campus Nord, Módul B4, 08034 Barcelona, Spain
paolo.moretti@upc.edu
[2]Departament de Física Fonamental, Facultat de Física, Universitat de Barcelona
Av. Diagonal 647, 08028 Barcelona, Spain
[3]IRCC – Institute for Cancer Research and Treatment
Strada Provinciale 142, Km. 3.95, 10060 Candiolo (Turin), Italy

Experimental studies have gathered evidence that plastic flow proceeds through intermittent spikes of activity, which extend over multiple spatial and temporal scales [1,2]. A fundamental question is whether such avalanche-like behavior extends to nanoscale systems, where boundary effects may prove just as important as the bulk behavior of interacting dislocations. We address the issues of mechanics at the nanoscale, by providing a theoretical study of the mechanisms of yield and plastic flow in intrinsically small systems. We propose a simple geometry, reproducible in experiments on two-dimensional micrometer colloidal crystals and able to provide input for mechanical testing of crystalline thin films below the micro-scale. To this end, we perform atomistic simulations of uniaxially compressed crystals and investigate the size-scaling of the yield stress and the statistics of plastic-event sizes. We find that at these scales, the yield point depends on the system size in an anomalous non-power law fashion and is heavily affected by the shape, or aspect ratio, of the sample under examination. By means of elasticity theory, we provide an estimate of the yield stress, based on the surface interactions of dislocations. Our analytical prediction is found in good agreement with simulation results, suggesting that at the nanoscale boundary effects are integral to the problem of plasticity, and not just peripheral to dislocation bulk behavior. Surprisingly, in the flow stage deformation still proceeds through avalanches extending over several scales, in spite of being mediated by a small number of dislocations. The scaling behavior of the energy dissipated in each event appears however substantially different from the universal power-law decay observed in larger systems, indicating that a novel theoretical framework is required to explain plastic flow at the nanoscale.

[1] D. M. Dimiduk et al., Science 312, 1188 (2006).
[2] M. Zaiser, Adv. Phys. 55, 185 – 245 (2006).

Fracture of disordered fuse networks with quenched plasticity

Phani Nukala[1], Pallab Barai[1], Rahul Sampath[1], Stefano Zapperi[2,3], and Mikko Alava[4]

[1]Oak Ridge National Laboratory, Oak Ridge, TN 37831-6164, USA
[2]CNR-IENI, Via R. Cozzi 53, 20125 Milano, Italy
[3]ISI Foundation, Viale S. Severo 65, 10133 Torino, Italy
[3]Department of Engineering Physics, Aalto University, FIN-02015 Aalto, Finland

We study scaling of fracture properties and crack roughness in disordered materials with randomly distributed perfect plastic and brittle phases. Many materials including those of natural biomaterials such as nacre are composed of brittle and perfectly plastic components at their microstructural level. Our study presents an algorithm that enables us to simulate fracture of such materials, and understand why such materials exhibit superior fracture toughness.

Latest advances in the development of the Adaptive Resolution Scheme

Simon Poblete[1], Sebastian Fritsch[1] , Kurt Kremer[1] and Luigi Delle Site[1]

[1]Max-Planck-Institut fuer Polymerforschung, Ackermannweg 10, D-55128 Mainz, Germany
poblete@mpip-mainz.mpg.de

The Adaptive Resolution Scheme (AdResS) [1] allows the performance of molecular dynamics simulation of a system divided into domains of different degree of resolution, through which particles can freely diffuse. Thermodynamic consistency can be assured through the application of the *thermodynamic force* [2], which is an external field that is able to guarantee thermodynamic equilibrium and remove previously reported artifacts [1].
Here, we present the latest advances on the development of this method and its applications.

[1] M. Praprotnik, L. Delle Site and K. Kremer, J. Chem. Phys. 123, 224106 (2005).
[2] S. Poblete, M. Praprotnik, K. Kremer and L. Delle Site, J. Chem. Phys. 132, 114101 (2010).

From an atomistic to a path integral representation of molecules in adaptive simulation

Adolfo Poma[1] and Luigi Delle Site[2]

[1,2]Max Planck Institute for Polymer Research, Ackermannweg 10, D-55128 Mainz, Germany, dellsite@mpip-mainz.mpg.de

Simulations that couple different classical molecular models in an adaptive way by changing the number of degrees of freedom on the fly are currently made within a reasonably consistent theoretical framework. The same does not occur when it come to classical-quantum adaptivity. The main reason for this is the difficulty in describing a continuous transition between the two different kind of physical principles: probabilistic for the quantum and deterministic for the classical. Here we report an algorithm [1] to perform an adaptive representation of molecules from a classical to a quantum description in a continuous and smooth way. It employs the path integral (PI) description of atoms; this latter maps the quantum nature of the atoms onto an effective classical model describing it as a classical polymer ring. In this way the process of interfacing adaptively a quantum region to a classical one translates into the full classical problem of interfacing two regions with a different number of "*classical*" degrees of freedom. Our approach captures the quantum delocalization of particles, which mainly affects the static properties in liquids as we show for a model system of tetrahedral molecules. A coarse grained (CG) procedure was used to reduce the large number of degrees of freedom of PI description to one effective CG site, later this effective model is coupled to the PI through the AdResS method [2-4]. Our implementation preserves the thermodynamic equilibrium among the two descriptions(PI/CG) allowing the free diffusion of molecules from one region to another.

[1] A.B.Poma and L. Delle Site, see arXiv:1002.4118v1 [cond-mat.soft] (2010).
[2] M. Praprotnik, L. Delle Site and K. Kremer, J. Chem. Phys. 123, 224106 (2005).
[3] C. Junghans, M. Praprotnik and L.Delle Site, in "Multiscale Simulation Methods in Molecular Sciences", NIC Series, Vol. 42, pg. 359 (2009).
[4] S. Poblete, M. Praprotnik, K. Kremer and L. Delle Site, J. Chem. Phys. 132, 114101 (2010).

A three-dimensional Continuum Theory of Dislocations - Modelling and Application to a Composite

Stefan Sandfeld[1], Thomas Hochrainer[2], Peter Gumbsch[1, 3] and Michael Zaiser[4]

[1]Karlsruhe Institute of Technology, izbs, Engelbert-Arnold-Str. 4, 76131 Karlsruhe, Germany
[2]Department of Scientific Computing, Florida State University, Tallahassee, FL 32310, USA
[3]Fraunhofer IWM, Wöhlerstr. 11, 79108 Freiburg, Germany
[4]School of Engineering, Institute for Materials and Processes, The University of Edinburgh, King's Buildings, Sanderson Building, Edinburgh EH9 3JL, United Kingdom

stefan.sandfeld@kit.edu

The increasing demand for materials with well-defined micro-structure, accompanied by the advancing miniaturisation of devices is the reason for a high demand for physically motivated, dislocation-based continuum theories of plasticity. Only recently rigorous techniques have been developed [1] for performing meaningful averages over systems of moving, curved dislocations, yielding evolution equations for a higher order dislocation density tensor. This *Continuum Dislocation Dynamics* Theory (CDD) was recently applied to various benchmark problems and applications in confined plasticity [2].

Here, CDD is applied to a composite material with elastic inclusions which are embedded into a plastically deforming matrix. The results are compared with those of various non-local crystal plasticity models and DDD simulations found in literature [3]. While [3] considers only straight, parallel edge dislocations, CDD allows for generalising the planar system towards a three-dimensional system where dislocations may have arbitrary orientation and curvature. By including curvature, the theory naturally accounts for deformation-induced increases in the overall dislocation density without having to invoke ad-hoc assumptions about dislocation sources. The hardening behaviour of both models as well as the evolution of total and 'geometrically necessary' dislocation density are discussed.

References

[1] T. Hochrainer, M. Zaiser, P. Gumbsch, A three-dimensional continuum theory of dislocations: kinematics and mean-field formulation, Phil. Mag. 87, 1261-1282 (2007)

[2] S. Sandfeld, T. Hochrainer, P. Gumbsch, M. Zaiser, Numerical Implementation of a 3D Continuum Theory of Dislocation Dynamics and Application to Microbending, to be published in Phil. Mag.

[3] Bittencourt, E.; Needleman, A.; Gurtin, M. and Van der Giessen, E. ,A comparison of nonlocal continuum and discrete dislocation plasticity predictions, JMPS 51, 281-310 (2003)

Micro-structure Evolution under torsional loading in Single Crystals: a Comparative Study of Discrete and Continuous Dislocation Simulations

Stefan Sandfeld[1], Jochen Senger[1], Thomas Hochrainer[2], Daniel Weygand[1], Michael Zaiser[3] and P. Gumbsch[1,4]

[1]Karlsruhe Institute of Technology, izbs, Engelbert-Arnold-Str. 4, 76131 Karlsruhe, Germany
[2]Department of Scientific Computing, Florida State University, Tallahassee, FL 32310, USA
[3]School of Engineering, Institute for Materials and Processes, The University of Edinburgh, King's Buildings, Sanderson Building, Edinburgh EH9 3JL, United Kingdom
[4]Fraunhofer IWM, Wöhlerstr. 11, 79108 Freiburg, Germany

stefan.sandfeld@kit.edu, jochen.senger@kit.edu

The evolution of the dislocation micro-structure of a thin single crystalline FCC wire under torsional loading is studied by means of *Discrete Dislocation Dynamics* simulations (DDD) [1] and compared to results from *Continuum Dislocation Dynamics* Theory (CDD) [2]. Since CDD is based on a higher-order dislocation density tensor we show how discrete dislocation ensembles can be 'converted' into a continuous dislocation density description by a higher-order averaging procedure. The concomitant loss of information is critically analysed with regard to comparability of both (DDD and CDD) models.
Torsion of a wire is a particularly instructive example for such a comparison since geometrically necessary dislocations evolve systematically with the imposed torsion angle and resulting dislocation micro-structure [3].

References

[1] D. Weygand, P. Gumbsch, *Study of dislocation reactions and rearrangements under different loading conditions*, Mat. Sci. Eng. A 400 (2005) 158-161

[2] T. Hochrainer, M. Zaiser, P. Gumbsch, *A three-dimensional continuum theory of dislocations: kinematics and mean-field formulation*, Phil. Mag. 87 (2007), 1261-1282

[3] N. A. Fleck, G.M. Muller , M.F. Ashby, and J.W. Hutchinson, Strain gradient plasticity - theory and experiment, Acta Metall. 42 (1994), 475-487

Ordering Icosahedral Network System in Relaxation Process of Amorphous Metals

Yoji Shibutani[1], Masato Wakeda[2], Daisuke Matsunaka[1]

[1]Department of Mechanical Engineering, Osaka University, 2-1, Yamadaoka, Suita, Osaka, 565-0871, sibutani@mech.eng.osaka-u.ac.jp;
[2]Department of Mechanical Engineering, Iwate University, 4-3-5, Morioka, Iwate, 020-8551.

ABSTRACT

Relaxation process of amorphous metals is thermodynamic competition between disordering and crystallization spatially and temporally. Several cooperative interactions among the short-range and the middle-range neighbors produce two characteristic relaxations, so called alpha- and beta-relaxations. Through such a complex process, the formed icosahedral internal structure of, for example, Zr-base amorphous metal determines the glass stability, and also global elastic properties and irreversible plastic deformability. Recently, the discussion on the isolated-imaged icosahedral atomic structure has been extended to the ordering one with larger length scale, that is, the middle-range order. The present study focuses on the formation mechanism of icosahedral network system of Cu-Zr binary amorphous model constructed by the rapid quenching in the framework of molecular dynamics simulations. Voronoi polyhedra analyses expose a fact that the icosahedra do not randomly distribute in space but form the characteristic inter-penetrating icosahedral clustering. The formation process is quantified using simple network theory to describe how these icosahedra link together in the relaxation process. It is also found that the highly developed inter-penetrating icosahedral clusters have much higher local elastic moduli than those of independently existing icosahedra and the other polyhedra.

1. Introduction

Bulk metallic glasses (BMGs) have high glass forming ability and hence the large-sized bulk of a cylinder or a plate can successfully be realized. Their high strength, high fracture toughness and high corrosion resistance, which are essentially attributed to the disordered atomic configuration, have already been reported. In these days, there have been considerable interests in their medium-range ordering (MRO), which probably affects the mechanical deformability linked to Young's modulus in the infinitesimal deformation and also shear banding resistance in the finite one. Some MRO model ideas have been suggested by the experimental and computational studies [1-4], and among them, the atomic cluster model made of inter-penetrating icosahedra might be one of the prospective candidates. To our knowledge, such analyses can go back more than two decades. Tomida & Egami have investigated orientation order of inter-penetrating icosahedral cluster in liquids and glasses by molecular dynamics (MD) simulations, and discussed its influence on the glass transition in detail [5]. In recent years, Shimono & Onodera [3,6] and Wakeda & Shibutani [7] have shown the existence of both icosahedral short-range ordering (SRO) and network-like MRO composed of the icosahedra in the supercooled liquid and also in the glass state of metals. Moreover, *ab initio* MD, which gives us a more physically reliable interaction, has shown that there are vertex shared and inter-penetrating (intercrossed) icosahedral MROs in the metallic glasses [4].

In the present research, the relationship between development of icosahedral clustering in the relaxation process and enhancement of elastic rigidity due to it is focused. We first investigate the morphological features characterized by both Voronoi technique, which has been modified to be applicable to the size difference of components [8], and the parameter used in the network science. Moreover, the atomic-level elastic constants, which consider only the potential energy contribution, are estimated to that the icosahedral MRO structures as one of the basic mechanical properties, and then the discussions on their morphological and mechanical relation are qualitatively carried out.

2. Atomic amorphous model

$Cu_{57}Zr_{43}$ binary amorphous model, containing about 30,000 atoms, was constructed via quenching process. The interatomic potentials employed here are the empirical ones suggested by Kobayashi, et al. [9], which refer two-body effects. Totally, three kinds of potential parameter sets are prepared to describe Cu-Cu, Cu-Zr and Zr-Zr interactions. The alloy model was quenched and relaxed as follows. First, a randomly packed initial state was numerically heated up to 2000 K. After a sufficient relaxation of 20 ps, the model was cooled down to 0 K at a rate of 10^{12} K/s. The external pressure during this heat treatment was kept at zero by the Parrinello-Rahman ensemble, and the temperature of the whole cell was controlled by scaling the velocities of atoms. Periodic boundary conditions were applied to three-dimensional directions in order to eliminate inhomogeneous surface effects. The details on this treatment have been given in the previous reference [10].
The glass transition temperature T_g is roughly around 850 K, because the volume-versus-temeperature curve changes its gradient explicitly. For the present atomic composition (Cu: 0.57 and Zr: 0.43), it is difficult to imagine the corresponding perfect crystalline model. Therefore, we cannot obtain the precise melting point, which is an important information to recognize whether it is a supercooled state or not. Alternatively, as shown in Fig. 1, we performed a heating process simulation for a Zr_2Cu crystalline model with C11b structure constructed using the same potentials. You can see the melting temperature around 2400 K and then this condensed matter is passed at glass transition temperature around 950 K. This means that the above maximum heating temperature of 2000 K for $Cu_{57}Zr_{43}$ could be in the supercooled liquid state in the framework of computational model.

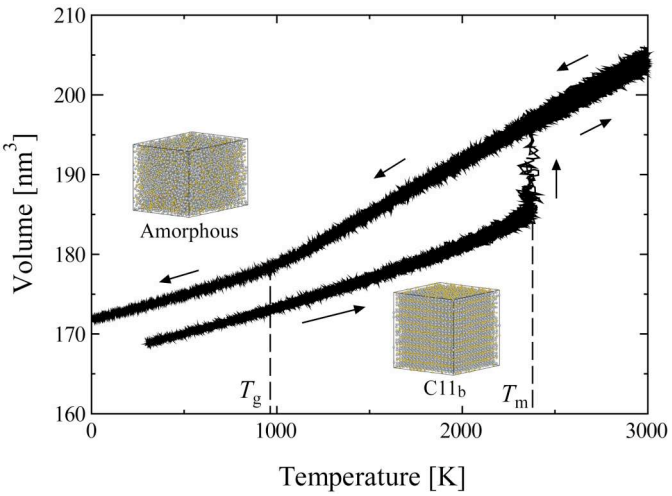

Figure 1. Heat treatment from crystals of Zr_2Cu to amorphous $Zr_{67}Cu_{33}$.

3. Formation of inter-penetrating icosahedral cluster

Icosahedral configuration is composed of one center and twelve neighbor atoms and it is characterized by five-fold symmetry, which never attains the spatial periodicity. It is suggested that the stable icosahedral order in the supercooled liquid prevents a formation of long-range crystalline order, resulting in the enhancement of glass forming ability. For example, Shintani & Tanaka has recently indicated that a frustration between the icosahedral SRO and the crystalline order controls the glass forming ability of liquids [11]. Analogously, the fully developed icosahedral MRO might stunt a nucleation and growth of crystalline nucleus.

Using the fully relaxed amorphous model, Voronoi polyhedron analysis gets more than hundreds of types of polyhedra, among which the most popular polyhedron corresponds to the icosahedral atomic configuration. Examples of the icosahedral atomic configuration and the characteristic atomic clusters due to inter-penetrating icosahedra observed in the present model are shown in Fig. 2. A bond connecting center atoms of inter-penetrating icosahedra is here called "icosahedral bond (the number of icosahedral bonds is denoted as n_B)" as shown in Fig. 2 (b). The large n_B implies the existence of highly developed inter-penetrating icosahedral cluster such as Fig. 2 (h) and the structure even having up to nine icosahedral bonds (n_B=9) is surprisingly observed in the present model.

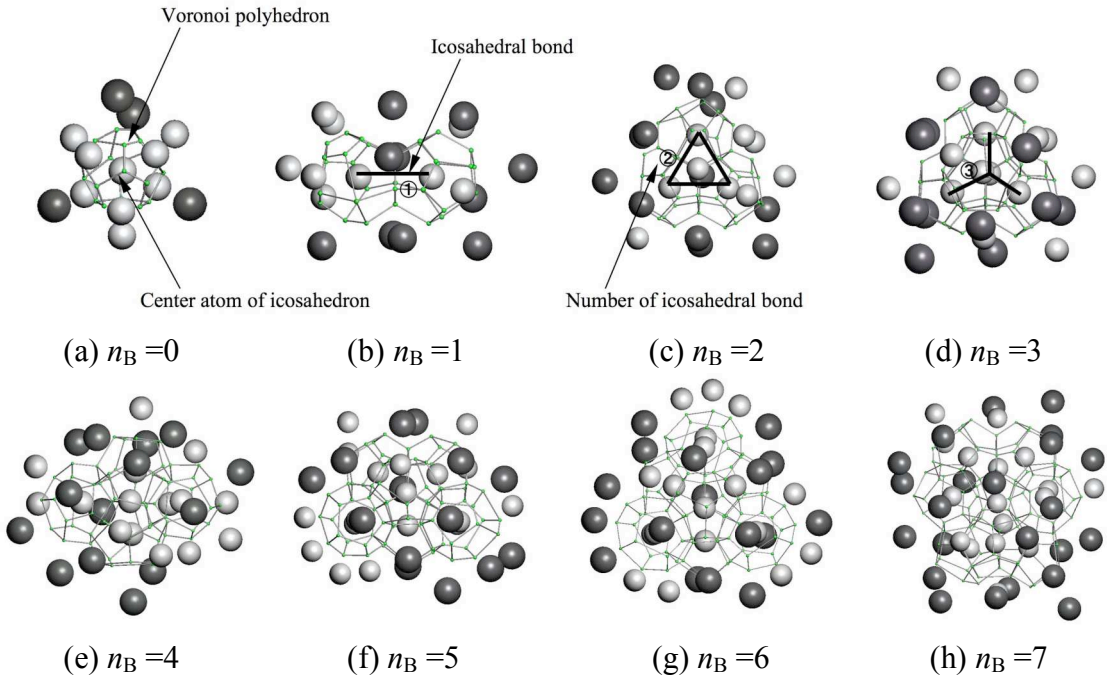

Figure 2. Icosahedral atomic configuration ((a)) and the characteristic atomic clusters constructed by inter-penetrating icosahedra ((b)-(h)). Light-colored atoms represent Cu, while darker ones represent Zr. The numbers inserted into the figures ((b) to (d)) stand for the icosahedral bond number n_B.

As has already reported in the some studies [3,5,12], the viewpoint from the whole system reminds that inter-penetrating icosahedra is the part of network-like structure (called "icosahedral network" [3]), as shown in Fig. 3. Only the center atoms of the linked inter-penetrating icosahedra and their bonds are depicted in the whole computational cell with 8 nm by 8 nm by 8 nm. As an example, one of the largest icosahedral clustering network existing there is 88 center atoms of icosahedra which are continuously connected by the icosahedral bonds with the size of about 4 nm by 2 nm by 2 nm. Similar to the Shimono's results [3], we can confirm that one typical characteristic of the icosahedral network is a "triangular geometry" composed of three icosahedra and the corresponding number of icosahedral bonds.

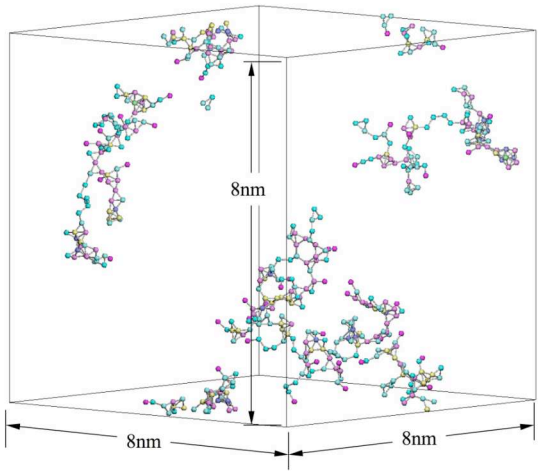

Figure 3. Network structure consisting the inter-penetrating icosahedra. For simplicity, the network is visualized by the center atom of icosahedron and icosahedral bond.

This unit is consecutively connected with like a chain, extending to a medium-range size.
In order to give the deeper insight into the characteristics of network structures, we employ a parameter of clustering coefficient X, ordinarily used in network science [13]. For the center atom of icosahedron α, it can be defined as follows;

$$X^{\alpha} = \frac{2L^{\alpha}}{n_{\mathrm{B}}^{\alpha}(n_{\mathrm{B}}^{\alpha}-1)} \tag{1}$$

where X^{α} and n_{B}^{α} are clustering coefficient and the icosahedral bond number according to icosahedron α, respectively. L^{α} is the number of triangular geometry which is assumed here as the basic unit of clustering. Clustering coefficient provides an effective indication of local clustering among icosahedra. We also calculate average clustering coefficient $\bar{X}$ of all icosahedra existing in the model. Based on both the icosahedral bond number n_{B} and the clustering coefficient X, any icosahedron is classified into one and three types: (a) isolated icosahedron, and icosahedron belonging to the network structure as a part of (b) chain, (c) triangular geometry, and (d) joint (hereafter, (a) "*isolate*", (b) "*chain*", (c) "*triangle*", (d) "*joint*", respectively), as shown in Fig. 4.

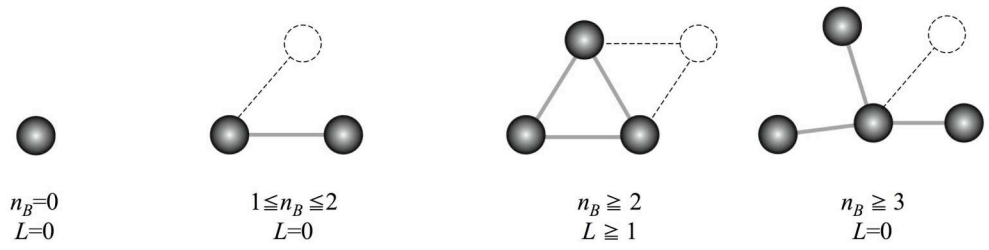

(a) Isolate (b) Chain (c) Cluster (d) Joint

Figure 4. One isolated icosahedron and three types of basic network structure according to the bond number and shape.

To certify the icosahedral network property, we construct an artificial network model with both the randomly selected atoms and their bonds (named as "random network"). If the spatial distribution of icosahedra is completely random without any specific rule, there may be no significant difference between the two. The random network model amenable to the probability theory is constructed as follows. First, from the atomic configurations that we investigate the icosahedral network, the same number of atoms as icosahedra are extracted randomly and named as "group R" (in the present model, the center atoms of icosahedron are

almost Cu, thus we extract only Cu atom). Then, if an atom of group R has "the nearest neighbor atom" (defined as an atom shearing the face of Voronoi polyhedron) that also belongs to the group, a bond between the two atoms is formed and named as "random bond". This bonding procedure for all atoms belonging to the group R is repeated until achieving the final random network model.

Summarizing the detailed differences in the network states of both models on the average bond number $\overline{n}_{\mathrm{B}}$, average clustering coefficient $\overline{X}$, and the proportions of bond state (i.e. *isolate*, *chain*, *triangle*, and *joint*), the icosahedral network has the averaged bond number of 2.57 and the averaged clustering coefficient of 0.397, which are approximately two times larger than those of the random network. Moreover, the icosahedral network is characterized by the large amount of triangle local structure, which supports the assumption of the triangle unit of the networking.

For network formation during cooling process from liquid, we also investigate the icosahedral and the random network structures using the same procedures as mentioned above. To remove the thermal fluctuation at the relatively high temperature, time averaging is fully taken. First, we extracted atomic configurations from the model in a quenching process at 1900K, 1800K, ・・・, 200K, 100K. Then, at each temperature, the atomic configurations were individually relaxed for 10,000 MD steps under NPT ensemble. During the relaxing process, 100 snapshots of atomic system of the icosahedral and the random networks are taken up for every 100 steps, and then averaged, respectively. The results are summarized in Fig. 5 where the histories of the clustering coefficient $\overline{X}$ and the fraction of bond states change during the cooling process are shown. Comparing with the artificial random network model provides us deeper comprehension of distinguishing networking process of icosahedra, and, in brief term, the icosahedral network model exhibits the stronger networking tendency for almost twice than the random network model.

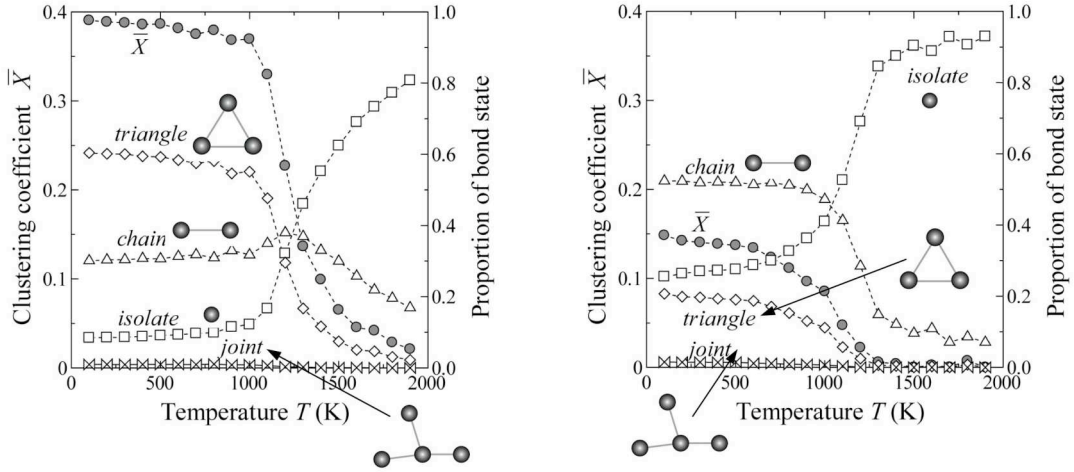

(a) Icosahedral network (b) Random network

Figure 5. Clustering coefficient and proportion of bond state during cooling process from liquid. At each temperature, two network models have exactly the same number of atoms that construct the network.

4. Local elastic moduli of icosahedral cluster

Our previous study [10] focusing on the relationship between the internal geometrical structure and the mechanical properties of the whole system concluded that the model with the higher occupied ratio of icosahedra has the higher rigidity. That leads a presumption that the local atomic packing state with low "free volume", which is offen referred as the atomic

packing state, may be attributed to high elastic resistance. In the present contribution, the atomic-level elastic moduli is dicussed in relation to icosahedral clustering. In order to simplify their estimations, they are calculated using only the potential energy contribution by neglecting the stress fluctuation and the kinetic energy contributions in the fluctuation formula [14]. That is,

$$C_{ijkl}^{\alpha} = \frac{1}{\upsilon^{\alpha}} \left\{ \sum_{\beta(>\alpha)} \left(\phi'' - \frac{\phi'}{r^{\alpha\beta}} \right) \right\} \frac{r_i^{\alpha\beta} r_j^{\alpha\beta} r_k^{\alpha\beta} r_l^{\alpha\beta}}{(r^{\alpha\beta})^2} \quad , \tag{2}$$

where C_{ijkl}^{α} (i, j, k, l =1, 2, 3) and υ^{α} are a component of elastic constants and atomic volume of atom α, r^{α} is the distance between atom α and β. ϕ' and ϕ'' are the first and second order deviatetes of two-body interatomic potential used in this study. Since C_{ijkl}^{α} reduces to be that at 0K, the amoprhous model fully relaxed by conjugate gradient technique was provided for calculations of Eqn. (2) with no time averaging. Voigt notation of C_{IJ} (I, J =1, 2, ... , 6) will be used afterwards. We should notify that the calculation of Eqn. (2) involves some intrinsic errors on estimating atomic volume υ^{α}, especially, for the multi-component alloys. The weighted Voronoi technique [8] employed here helps to reduce the error as much as possible. Remind that the two-body potential theoretically holds the Cauchy relation that C_{12} is equal to C_{44}. Thus, the representative elastic constants obtained here are only two. Relations between the two components and the coordination number and the icosahedral bond are shown in Fig. 6. As seen there, most packing state of icoahedron produces the highest moduli and also they are significantly increasing as the number of icosahedral bonds.

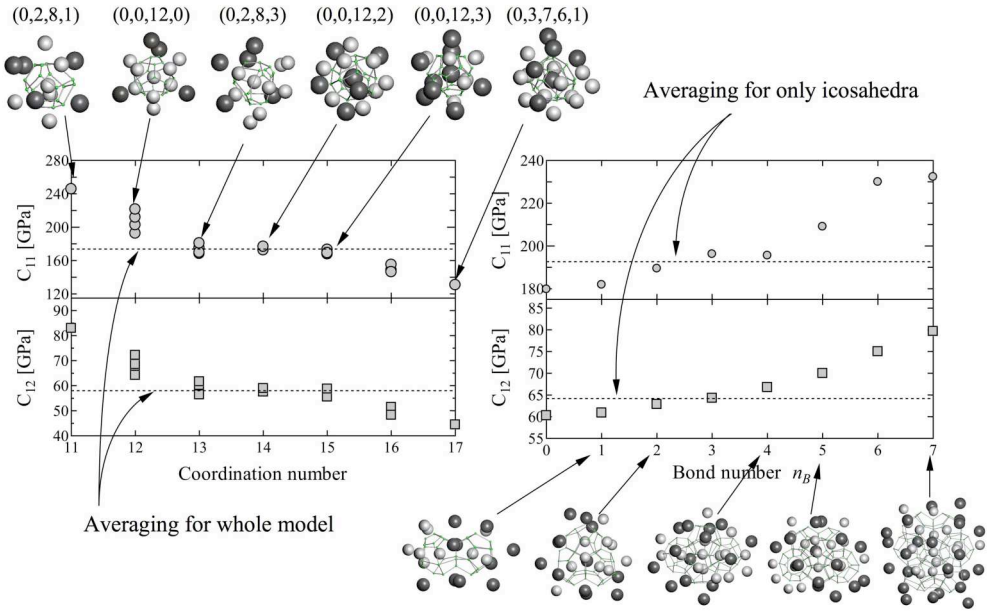

(a) C_{IJ} versus coordination number (b) C_{IJ} versus the number of icosahedral bonds

Figure 6. Atomic-level elastic constants of C_{11} and C_{12} versus the coordination number and the number of icosahedral bonds.

Moreover, since the icosahedra configurations distribute toward a random orientation in the model, we introduce the averaging procedure according to the polyhedron orientation; C_{11}^{*} comes from averaging of C_{11}, C_{22}, and C_{33}, and C_{12}^{*} does from C_{12}, C_{23}, C_{31}, C_{44}, C_{55}, and C_{66} based on the Cauchy relation mentioned above. The calculated elastic modulus C_{12}^{*} of each center atom of icosahedron varies widely, ranging from 20 GPa to 120 GPa, because each icosahedron is situated at the entirely different stress and strain states. Meanwhile, averaging

C_{11}^* and C_{12}^* of all center atoms of only icosahedra are 192.7 GPa and 64.2 GPa, respectively (both are dashed lines in Fig. 5 (b)), which are slightly larger than those of whole model (C_{11}^* = 173.8 GPa and C_{44}^* = 58.0 GPa; both are dashed lines in Fig. 5 (a)). The continuous isotropic material has the well-known relation of $2C_{44}=C_{11}-C_{12}$. Applying the atomic-level but orientation averaged elastic constants for the whole model, you can see easily find that this isotropic relation fairly holds. That is, the present amorphous atomic system with locally inhomogeneous packing is globally isotropic. The result indicates that the densely packed local structure tends to have the higher elastic rigidity, and thus gives a good account of our previous result [10] from the atomistic viewpoint.

5. Summaries

MD simulations were performed using the Cu-Zr binary amorphous model to find out the characteristic medium-range order structure. It is confirmed from the detailed analyses during cooling process from the assumed supercooled liquid state that icosahedral structure forms the mutual inter-penetration among the preexisted icosahedra, leading to the characteristic network structures in the glass state. Moreover, it is obtained that the atomic-level elastic moduli of center atom of the icosahedral cluster increase with the number of icosahedral bonds, indicating that the highly developed inter-penetrating icosahedral cluster has the much higher elastic rigidity.

Acknowledgements
The author (YS) gratefully acknowledges the financial support from MEXT, Japan, Grants-in-Aid for Scientific Research (S) (20226004).

References
[1] Miracle D B, Nature Mat., 3, 2004, pp.697.
[2] Sheng H W, Luo W K, Alamgir F M, Bai J M, Ma E, Nature, 439, 2006, pp.419.
[3] Shimono M, Onodera H, Mat. Sci. Forum, 539-543, 2007, pp.2031.
[4] Hui X, Gao R, Chen G L, Shang S L, Wang Y, Liu Z K, Phys. Lett. A, 372, 2008, pp.3078.
[5] Tomida T, Egami T, Phys. Rev. B, 52, 1995, pp.3290.
[6] Shimono M, Onodera H, Mater. Sci. Eng. A, 449-451, 2007, pp.717.
[7] Wakeda M, Shibutani Y, Acta Mat., 58, 2010, pp.3963.
[8] Park J, Shibutani Y, Mat. Trans., 47, 2006, pp.2904.
[9] Kobayashi S, Maeda K,Takeuchi S, Acta Metall., 28, 1980, pp.1641.
[10] Wakeda M, Shibutani Y, Ogata S, Park J, Intermetallics, 15, 2007, pp.139.
[11] Shintani H, Tanaka H, Nature, 2, 2006, pp.200.
[12] Jónsson H, Andersen H C, Phys. Rev. Lett., 60, 1988, pp.2295.
[13] Watts D J, Strogatz S H, Nature, 393, 1988, pp.440.
[14] Ray J R, Garden H W, Mol. Phys., 43, 1981. pp.1293.

Effective Coefficients of Quasi-Stationary Maxwell's Equations with Multiscale Isotropic Random Conductivity

O.N. Soboleva[1], **E.P. Kurochkina** [2]

[1]**Institute of Computational Mathematics and Mathematical Geophysics, pr. Lavrentieva, 6, 630090 Novosibirsk, Russia, E-mail address: olga@nmsf.sscc.ru**
[2]**Institute of Thermophysics, 630090 Novosibirsk, Russia**

ABSTRACT

In this paper we present effective coefficients in quasi-stationary Maxwell's Equations for a multiscale isotropic medium. The conductivity is mathematically represented by Kolmogorov's multiplicative continuous cascade with a lognormal distribution of probability. The size of solution domain of the problem is considered to be large as compared with the size of heterogeneities of the medium. For solving the problem we use a subgrid modeling approach. The theoretical result is compared to the results of the direct 3D numerical modeling and to the results of conventional perturbation theory.

1. Introduction

The main aim of the electromagnetic logging is to estimate formation resistivities as correctly as possible. At the mathematical modeling of the electromagnetic logging problems the large-scale details (layers, big rock intercalations) are described in mathematical models with help of the boundary conditions. The small-scale details of parameters are as a general rule unknown. They should be taken into account within the statistical approach, introducing effective parameters and finding simplified models with computationally resolvable scales, whose solutions are sufficiently close to the solutions of original full equations. Such simplified models, without too small scales, which are built on mathematical model of full equations with the computationally unresolved scales, are referred to as subgrid modeling. Most of oil and gas reservoirs are extremely heterogeneous since their frame is made up of minerals of multicomponent composition with a complicated structure of porous channels. So, field measurements of electric conductivity, permeability, porosity, have shown that the bounds of heterogeneity increase as scale of observation is increased. In order to use the subgrid modeling or the functional renormalization method it is necessary that the problem has some "scale regularity". It is conceivable that many problems, in fact, do have such a regularity. A combination of irregular, heterogeneous parameters and a systematic increase of irregularity with scale have led researchers to apply fractal concepts [1]. We represent a multiplicative continuous cascade for modeling electric conductivity, which allows us to bring in a correct small-scale smoothing procedure and to obtain effective coefficients for the estimation of the first and the second statistical moments of the electric or magnetic field strengths, current density in the quasi-stationary Maxwell's equations. The simplest method of obtaining effective parameters and simplified models uses perturbation theory. The solution of differential equations can be sought as a perturbation series in powers of a small parameter, for example conductivity. The subsequent procedure of averaging each term of the series at the given statistics of conductivity fluctuations enables one to find the average electric or magnetic field strengths, the average current density and, finally, to calculate the effective conductivity. But all the statical moments of geophysical parameters are as a rule unknown so one uses the lowest approximation of perturbation theory. The theoretical result obtained by subgrid modeling is compared to the results of the direct 3D numerical modeling

and to the results of conventional perturbation theory.

2. Statement of the problem

Let quasi-stationary conditions in a medium be satisfied. According to[?], the quasi-stationary approximation of Maxwell's equations for monochromatic fields $\widetilde{\mathbf{E}}(\mathbf{x},t) = Re\left(\mathbf{E}(\mathbf{x})\, e^{-i\omega t}\right)$, $\widetilde{\mathbf{H}}(\mathbf{x},t) = Re\left(\mathbf{H}(\mathbf{x})\, e^{-i\omega t}\right)$ in the absence of extraneous currents can be written as

$$\begin{aligned} rot\mathbf{H}(\mathbf{x}) &= \sigma(\mathbf{x})\,\mathbf{E}(\mathbf{x}), \\ rot\mathbf{E} &= i\omega\mu\mathbf{H}, \end{aligned} \tag{1}$$

where $\mathbf{E}$ and $\mathbf{H}$ are vectors of the electric and magnetic field strengths; μ is magnetic permeability; $\sigma(\mathbf{x})$ is electric conductivity; ω is cyclic frequency; and $\mathbf{x}$ is the vector of spatial coordinates. Practically, for all the rocks except for rock with inclusion of ferromagnetic minerals the magnetic permeability is equal to the magnetic permeability of vacuum. We assume that $\mathbf{E}$, $\mathbf{H}$ are defined by a monochromatic source and the electric conductivity is constant outside of the finite volume V with a sufficiently smooth surface S. At the boundary of S, the tangent components of electric and magnetic field strengths are continuous. Let the field of electrical conductivity is measured in small steps of l_0 at each point $\mathbf{x}$. A random function of spatial coordinates $\sigma(\mathbf{x})$ is considered as a limit $\sigma(\mathbf{x})_{l_0}$ at $l_0 \to 0$. The dependence of $\sigma(\mathbf{x})$ on the scale l_0 is considered as a factor that allows us to develop new approaches to the investigation of a randomly heterogeneous medium [2]:

$$\sigma_{l_0}(\mathbf{x}) = \sigma_0 \exp\left(-\int_{l_0}^{L} \varphi(\mathbf{x}, l_1)\frac{dl_1}{l_1}\right), \tag{2}$$

where σ_0 is constant. It is assumed that the electric conductivity has heterogeneities of scale l_1 from the range (l_0, L), where l_0 and L are minimal and maximal scales of measurements. We suppose that isotropic field $\varphi(\mathbf{x}, l)$ has a normal distribution, a statistically homogeneous correlation function $< \varphi(\mathbf{x},l)\,\varphi(\mathbf{y},l') > - < \varphi(\mathbf{x},l) >< \varphi(\mathbf{y},l') >= \Phi(|\mathbf{x}-\mathbf{y}|, l, l')\delta(\ln l - \ln l')$. Here the angle brackets denote the ensemble average. For the conservative cascade model $< \sigma_l(\mathbf{x}) >= \sigma_0$ should be satisfied for any scale l. Such a condition is satisfied when $\Phi_0(l) = 2 < \varphi(l) >$, where $\Phi_0(l) = \Phi(0, l)$. The electric conductivity field (2) is the multifractal if the minimum scale l_0 tends to zero. The function $\sigma(\mathbf{x}) = \sigma(\mathbf{x})_{l_0}$ is divided into two components with respect to the scale l. The large-scale (ongrid) component $\sigma(\mathbf{x}, l)$ is obtained by statistical averaging over all $\varphi(\mathbf{x}, l_1)$ with $, l_0 < l_1 < l$, $l - l_0 = dl$, where dl is small. A small-scale (subgrid) component is equal to $\sigma'(\mathbf{x}) = \sigma(\mathbf{x}) - \sigma(\mathbf{x}, l)$:

$$\begin{aligned} \sigma(\mathbf{x},l) = \sigma_0 \exp\left[-\int_{l}^{L} \varphi(\mathbf{x},l_1)\frac{dl_1}{l_1}\right] \times \left\langle \exp\left[-\int_{l_0}^{l} \varphi(\mathbf{x},l_1)\frac{dl_1}{l_1}\right]\right\rangle, \\ \sigma'(\mathbf{x}) = \sigma(\mathbf{x},l)\left[\frac{\exp\left[-\int_{l_0}^{l}\varphi(\mathbf{x},l_1)\frac{dl_1}{l_1}\right]}{\left\langle \exp\left[-\int_{l_0}^{l}\varphi(\mathbf{x},l_1)\frac{dl_1}{l_1}\right]\right\rangle} - 1\right]. \end{aligned} \tag{3}$$

The large-scale (ongrid) components of electric and magnetic field strengths $\mathbf{E}(\mathbf{x}, l), \mathbf{H}(\mathbf{x}, l)$ are obtained as averaging solutions to equations system (1), in which a large-scale component of conductivity $\sigma(\mathbf{x}, l)$ is fixed and a small component $\sigma'(\mathbf{x})$ is a random variable. The subgrid components of the electric and of the magnetic field strengths are equal to $\mathbf{H}'(\mathbf{x}) = \mathbf{H}(\mathbf{x}) - \mathbf{H}(\mathbf{x},l)$, $\mathbf{E}'(\mathbf{x}) = \mathbf{E}(\mathbf{x}) - \mathbf{E}(\mathbf{x},l)$. Substituting relations for $\mathbf{E}(\mathbf{x}), \mathbf{H}(\mathbf{x})$ and $\sigma(\mathbf{x})$

into equation system (1) and average over a small-scale component:

$$\begin{aligned} rot\mathbf{H}\left(\mathbf{x},l\right) &= \sigma(\mathbf{x},l)\mathbf{E}\left(\mathbf{x},l\right)+\left\langle \sigma'\mathbf{E}'\right\rangle , \\ rot\mathbf{E}\left(\mathbf{x},l\right) &= i\omega\mu\mathbf{H}\left(\mathbf{x},l\right). \end{aligned} \tag{4}$$

The second term on the right hand side of the first equation of system (4) cannot be rejected without preliminary estimation since the this correlation may be substantial. The choice of the form of this term in (4) determines the subgrid model. This expression is estimated using perturbation theory. Subtracting system (4) from system (1), and, taking into account only the terms of first order of magnitude, we obtain the subgrid equations:

$$\begin{aligned} rot\mathbf{H}' &= \sigma\left(\mathbf{x},l\right)\mathbf{E}'+\sigma'\mathbf{E}\left(\mathbf{x},l\right), \\ rot\mathbf{E}' &= i\omega\mu\mathbf{H}'. \end{aligned} \tag{5}$$

The variable $\mathbf{E}\left(\mathbf{x},l\right)$ on the right-hand side of (5) is considered to be known, then using perturbation theory we obtain

$$\left\langle \sigma'E'_{\alpha}\right\rangle =\left(-\tfrac{1}{3}\Phi_0+\tfrac{2}{3}k^2\int\limits_0^{\infty}re^{ikr}\Phi\left(r,l\right)dr\right)\sigma\left(\mathbf{x},l\right)E_{\alpha}\left(\mathbf{x},l\right)\tfrac{dl}{l}, \tag{6}$$

where $r=|\mathbf{x}-\mathbf{x}'|$, $k^2=i\omega\mu\sigma(\mathbf{x},l)$, $k=(1+i)\sqrt{\omega\mu\sigma(\mathbf{x},l)/2}$. For definiteness, we select the value of the root at which $Re\,k>0,\ Im\,k>0$. In magnitude the integral term in (6) is small if $\omega\mu L^2\sigma(\mathbf{x},l)\ll 1$ [3]. Ignoring the integral term and substituting (6) into (4), we have

$$\begin{gathered} rot\mathbf{H}\left(\mathbf{x},l\right)=\left(1-\tfrac{\Phi_0}{3}\tfrac{dl}{l}\right)\left[1+\left(\tfrac{\Phi_0}{2}-\left\langle\varphi\right\rangle\right)\tfrac{dl}{l}\right]\sigma_0\exp\left[-\int_l^L\varphi(\mathbf{x},l_1)\tfrac{dl_1}{l_1}\right]\mathbf{E}\left(\mathbf{x},l\right), \\ rot\mathbf{E}\left(\mathbf{x},l\right)=i\omega\mu\mathbf{H}\left(\mathbf{x},l\right). \end{gathered} \tag{7}$$

It follows that accurate within second order of smallness with respect to dl we have $\sigma_{l0}=\sigma_0+\left(\frac{\Phi_0}{6}-\left\langle\varphi\right\rangle\right)\sigma_0\frac{dl}{l}$. Passing to the limit at $dl\to 0$ we obtain the equation

$$\frac{d\ln\sigma_{0l}}{d\ln l}=\frac{1}{6}\Phi_0\left(l\right)-\left\langle\varphi\right\rangle. \tag{8}$$

For the scale invariant media, effective equations have especially a simple form

$$\begin{aligned} rot\mathbf{H}\left(\mathbf{x},l\right) &= \left(\frac{l}{L}\right)^{\left\langle\varphi\right\rangle-\Phi_0/6}\sigma_l\left(\mathbf{x}\right)\mathbf{E}\left(\mathbf{x},l\right), \\ rot\mathbf{E}\left(\mathbf{x},l\right) &= i\omega\mu\mathbf{H}\left(\mathbf{x},l\right). \end{aligned} \tag{9}$$

In the same manner we obtain the effective coefficients for the first and second covariance tensor of electric field and of the current density.

3. Numerical modeling

The following numerical problem is solved in order to verify the formulas obtained above. We solve problem (1) in a cube with an edge L_0. Alternating the magnetic field with a cyclic frequency ω influences the conducting medium. In the calculation, we use the following dimensionless variables : $\mathbf{x}=\widehat{\mathbf{x}}/L_0,\ \sigma=\widehat{\sigma}/\sigma_0,\sigma_0=\left\langle\widehat{\sigma}\right\rangle,\ \mathbf{H}=\widehat{\mathbf{H}}/H_0,\ \mathbf{E}=(L_0\sigma_0/k_1H_0)\,\widehat{\mathbf{E}},\ k_1=L_0\sqrt{\mu\omega\sigma_0}$. Thus, the problem is solved in a cube having sides of unit length, with $\sigma_0=1$, $H_0=1$. Equations (1) in the dimensionless form are written as

$$\begin{aligned} rot\mathbf{H}\left(\mathbf{x}\right) &= k_1\sigma\left(\mathbf{x}\right)\mathbf{E}\left(\mathbf{x}\right), \\ rot\mathbf{E}\left(\mathbf{x}\right) &= ik_1\mathbf{H}\left(\mathbf{x}\right). \end{aligned} \tag{10}$$

On the boundary with vacuum $z = 0$, we consider that the strength of the external magnetic field is $\mathbf{H} = (0, H_y(z), 0)$, $H_y(z) = H_0$. The magnetic and electric fields beyond the cube and at its boundaries are as follows: $H_y = \exp\left(-k_1 z/\sqrt{2}\right) \exp\left(ik_1 z/\sqrt{2}\right)$, $H_x = H_z = 0$, $E_x = \exp\left(-k_1 z/\sqrt{2}\right) \exp\left(ik_1 z/\sqrt{2} - \pi/4\right)$, $E_y = E_z = 0$. The conductivity field is simulated by formula (2), where the integral in (2) is replaced by a finite-difference formula in which it is convenient to pass to logarithm to the base 2:

$$\sigma\left(\mathbf{x}\right)_l = \exp\left[-\ln 2 \int\limits_{\log_2 l_0}^{\log_2 L} \varphi\left(\mathbf{x}, \tau\right) d\tau \approx 2^{-\sum\limits_{i=-5}^{-3} \varphi(\mathbf{x}, \tau_i)\Delta\tau}\right]. \tag{11}$$

The constant Φ_0 in should be taken from experimental data for heterogeneous media. We used $\Phi_0 = 0.3$. For the solution of the Maxwell's equation (10) there was implemented a method based on a finite-difference scheme proposed by Lebedev V.I.(1964) and the decomposition method described in [4]. In Figure 1 the theoretical result is compared to the results of the direct 3D numerical modeling and to the results of conventional perturbation theory.

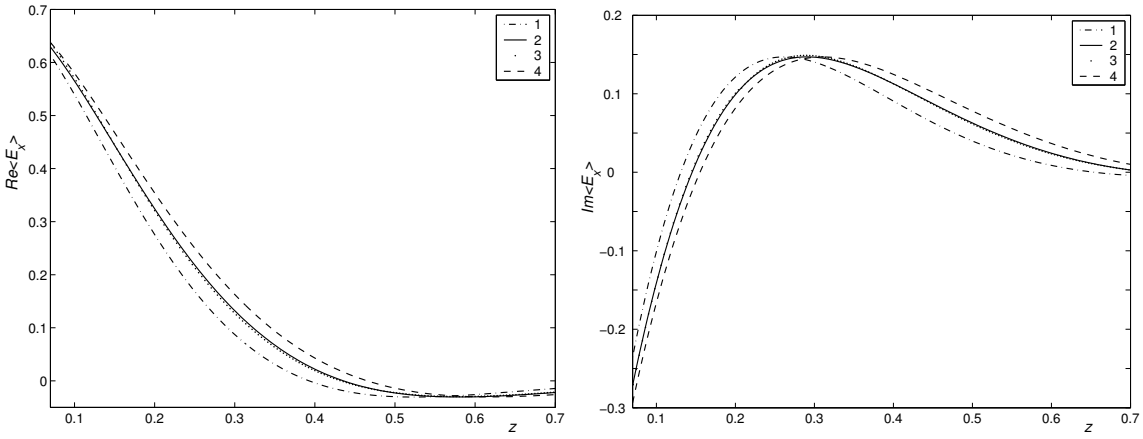

Figure 1: The average real and the average imaginary parts of component of the electric field strength along the x-axis. 1 – the result obtained for $\sigma = 1$; 2 – the result obtained by the effective system; 3 – the result of numerical modeling with σ calculated by model (11) for three scales, $\langle\sigma\rangle = 1$; 4 – the result obtained from conventional perturbation theory.

References

[1] Sahimi M. Flow phenomena in rocks: from continuum models, to fractals, percolation, cellular automata, and simulated annealing. *Reviews of Modern Physics*. **65**, 1393–1534, 1993.

[2] Kuz'min G.A., Soboleva O.N. Subgrid modeling of filtration in porous self-similar media. *J. Appl. Mech. Tech. Phys.* **43**, 583-592, 2002.

[3] Rytov S. M., Kravtsov Yu. A. & Tatarskii V. I. *Principles of Statistical Radiophysics*. **3, 4** Springer-Verlag, Berlin, 1987

[4] Davydycheva S., Drushkin V., Habashy T. An efficient finite-difference scheme for electromalnetic logging in 3D anisotropic inhomogeneous media. *Geophysics* . **68**, 1525–1536,2003.

Coupled continuum theory of dislocations and solute atoms

Ferenc Székely[1], István Groma and Géza Györgyi

[1] Eötvös University Budapest, Department of Materials Physics, PO BOX 32, 1518 Budapest, Hungary
e-mail[1]: szekely@metal.elte.hu

Groma et al. [1] have recently shown that the continuum equation governing the dynamical behaviour of a 2D dislocation system can be derived from a variational principle. An important feature of the variational approach is that it opens the possibility to incorporate additional material features, like grain boundaries, dislocation core properties, and the presence of solute atoms, into the continuum theory of dislocations. In the work presented, a phase field theory coupling dislocation and solute atoms is developed.

In order to formulate this theory one needs to add the free enthalpy of the solute atoms to the variational potential. Furthermore, the incorporation of appropriate terms accounting for dislocation core effect and interaction between dislocation and solute atoms is necessary. In the static case the well known Cottrel-atmosphere of solute atoms around dislocation is derived from the general theory. It was also shown that as it is known in the static case the effect of solute atoms can be taken into account by modified elastic constants.

Considering full dynamics, a well known feature of the dislocation-solute atoms system is the appearance of instabilities, like the Portevin-Le Chatelier effect. It is shown that the complete coupled dislocation solute atom model is able to account for the appearance of instabilities during creep in a given range of the parameters.

[1] Groma I, Györgyi G, Kocsis B, Dynamics of coarse grained dislocation densities from an effective free energy, Phil. Mag. 87, 1185-1199, (2007)

A scaling theory for size effects and strain bursts in microplasticity

Stefano Zapperi[1], Valentina Beato[2] and Micheal Zaiser[3]

[1]CNR-IENI, Via R. Cozzi 53, 20125 Milano, Italy.
[2]CNR-ISI, Via dei Taurini 19, 00185 Roma, Italy.
[3]Center for Materials Science and Engineering, University of Edinburgh, King's Buildings, Sanderson Building, Edinburgh EH93JL, UK.

Microcrystals deform very differently from their macroscopic counterparts, displaying a size-dependent yield stress and intermittent plastic strain bursts. Here we demonstrate that size effects and strain bursts are just two different signatures of fundamental collective phenomena that govern the dynamics of dislocation systems on all scales. We confirm the theory by demonstrating agreement between the results of 2D and 3D dislocation dynamics simulations and experimental results on compressed micropillars. Our results indicate that many peculiarities of small-sample plasticity may not depend on surface specific mechanisms.